

Surface spectral function in the superconducting state of a topological insulator

Lei Hao and T. K. Lee

Institute of Physics, Academia Sinica, NanKang, Taipei 11529, Taiwan

(Dated: January 13, 2013)

We discuss the surface spectral function of superconductors realized from a topological insulator, such as the copper-intercalated Bi_2Se_3 . These functions are calculated by projecting bulk states to the surface for two different models proposed previously for the topological insulator. Dependence of the surface spectra on the symmetry of the bulk pairing order parameter is discussed with particular emphasis on the odd-parity pairing. Exotic spectra like an Andreev bound state connected to the topological surface states are presented.

PACS numbers: 74.20.Rp, 73.20.At, 74.45.+c

I. INTRODUCTION

Recently, a new state of matter, the topological insulator, attracts much theoretical and experimental attention.[1, 2, 3, 4, 5, 6, 7, 8, 9, 10, 11, 12, 13, 14, 15] It has an electronic structure dominated by the spin-orbit coupling, which is a band insulator with a well-defined gap in the bulk but can host an odd number of Dirac cones protected by time reversal symmetry on the surface.[1, 2, 7] The intrinsic spin-orbit coupling makes it promising for spintronics applications.[10] The proximity induced superconducting state on the topological insulator surface by a deposited superconductor was proposed to create Majorana fermions[16], which may provide a new way to realize the topological quantum computation.[17, 18] Lately, the realization of a superconducting state in a typical topological insulator Bi_2Se_3 by intercalating Cu between adjacent quintuple units ($\text{Cu}_x\text{Bi}_2\text{Se}_3$) makes the system even more attractive.[19, 20] The large diamagnetic response shows that the pairing is mainly of bulk character. In another topological insulator Bi_2Te_3 , the application of a high pressure also turns the material into a superconducting state.[21, 22]

Since the superconductivity is bulk and intrinsic to the material, if zero energy surface Majorana fermion mode exists, it would be easier to manipulate as compared to that induced by proximity effect, as it would not experience the interface roughness or mismatch common to a junction type device. Possible nontrivial odd-parity pairing in $\text{Cu}_x\text{Bi}_2\text{Se}_3$ is proposed and analyzed by Fu and Berg.[23] It was argued that only if a bulk gap opens and the bulk pairing is odd in parity, would zero energy Andreev bound states appear in the surface spectrum. However, their analysis was concentrated on the case when the chemical potential is much larger than the gap and the topological surface states are already merged into the continuum conduction band. A similar analysis was put forward by Sato.[24]

Despite the above works, a detailed theoretical analysis of surface spectrum in the superconducting phase arising from a topological insulator is still lacking. In particular, not much is reported for the situation when the chemical potential is only slightly larger than the insulating

gap and both topological surface states (or, the surface conduction band[20]) and the continuum bulk conduction band are present but separated. Since the surface spectrum is central to the topological properties of a material both in the normal and in the superconducting state, which is also directly accessible by experimental techniques as ARPES[20] and STM[25], it is highly desirable to make a detailed study of them. This will help to understand better superconductivity in systems with nontrivial topological band structure.

We focus on two questions in this paper. One is the effect of superconducting pairing on the topological surface states[20] present in the normal state. The other is the existence of surface Andreev bound states. We have noticed that two different models[12, 26] are often used indiscriminatively in literature. They have the same normal state energy spectra but may be different in the superconducting state. We thus present our results for both of them. What happens to the topological surface states when pairing is introduced in the bulk depends on the orbital character of the topological surface state and on the bulk pairing symmetry. Only when the continuum part of the band opens a full gap and the topological surface states, while separated from the bulk conduction band, do not open a gap for an odd-parity pairing, would a gapless Andreev bound state appear. We find that the orbital characters of the topological surface states are different for the two models. For a certain bulk pairing symmetry, it is possible that the topological surface states of one model opens a gap while that of the other model is still intact. The existence of Andreev bound states, the most important indication of nontrivial topological order in the superconducting phase, is thus expected to be also related to the orbital character of the topological surface states. We show that the interplay between the continuum bulk conduction band and the topological surface states produces a ring or a segment of zero energy states in addition to the Andreev bound states depending on the symmetry of bulk pairing order parameters.

II. MODELS AND THE NORMAL STATE SURFACE MODES

In the following, when we talk about topological insulators, we would be mainly referring to Bi_2Se_3 , which shows a well defined Dirac cone structure for the topological surface states.[11, 12, 27] The model we consider below could be easily generalized to study other topological insulators like TlBiSe_2 [28, 29] and $\text{Bi}_2\text{Te}_2\text{Se}$ [30, 31].

The band structure of $\text{Cu}_x\text{Bi}_2\text{Se}_3$ is similar to that of Bi_2Se_3 , the most essential part of which consists of two p_z orbitals on the top and bottom Se layers hybridized with neighboring Bi p_z orbitals, in each quintuple Bi_2Se_3 unit.[12, 23] In the presence of spin-orbit coupling, the normal state has four degrees of freedom. Label the two orbitals concentrating mainly on the top and bottom (seeing along the $-z$ direction) Se layer of the various Bi_2Se_3 quintuple units as the first and second orbital, the basis is taken as $\psi_{\mathbf{k}} = [c_{1\mathbf{k}\uparrow}, c_{2\mathbf{k}\uparrow}, c_{1\mathbf{k}\downarrow}, c_{2\mathbf{k}\downarrow}]^T$. The models could be written compactly in the following matrix form[12, 23, 26]

$$H(\mathbf{k}) = \epsilon_0(\mathbf{k})I_{4 \times 4} + \sum_{i=0}^3 m_i(\mathbf{k})\Gamma_i. \quad (1)$$

$I_{4 \times 4}$ is the fourth order unit matrix, giving rise to a topologically trivial shift of the energy bands and would be neglected in most of our following analysis. In terms of the two by two Pauli matrices s_i ($i=0, \dots, 3$) in the spin subspace and σ_i ($i=0, \dots, 3$) in the orbital subspace, the first three Dirac matrices are defined as[12, 26] $\Gamma_0 = s_0 \otimes \sigma_1$, $\Gamma_1 = s_1 \otimes \sigma_3$, $\Gamma_2 = s_2 \otimes \sigma_3$. As regards Γ_3 , there are presently two different choices: (I) $s_0 \otimes \sigma_2$ [23, 26, 32] and (II) $s_3 \otimes \sigma_3$ [12, 33, 34, 35, 36], which define the two models that would be considered in parallel in the following discussion. Since Bi_2Se_3 is inversion symmetric, parity could be used to label states. Some papers adopt the bonding and antibonding states of the two orbitals defined above as the orbital basis.[12, 32, 33, 34, 35, 36] The corresponding models could be obtained in terms of a simple unitary transformation performed in the orbital subspace. Note that, the two different models give the same bulk band dispersion $\epsilon_{\pm}(\mathbf{k}) = \epsilon_0(\mathbf{k}) \pm \sqrt{\sum_{i=0}^3 m_i^2(\mathbf{k})}$, with each of two eigen-energies two fold Kramers degenerate due to the time reversal symmetry and the inversion symmetry of the model. However, we will show in the following that they are essentially two physically distinct models.

For the coefficients $\epsilon_0(\mathbf{k})$ and $m_i(\mathbf{k})$ ($i = 0, 1, 2, 3$), there are different possible parameterizations which coincide with each other close to the Γ point.[12, 14, 26, 37] Without loss of generality, we take the parameterizations of Wang *et al.*[26]. Since the diagonal term $\epsilon_0(\mathbf{k})$ proportional to the unit matrix does not affect the topological characters, it is ignored here. The system is defined on a hypothetical bilayer hexagonal lattice stacked along the z -axis, respecting the in plane hexagonal symmetry

of the original Bi_2Se_3 lattice. With the three independent in-plane nearest neighbor unit vectors defined as $\hat{b}_1 = (\frac{\sqrt{3}}{2}, \frac{1}{2})$, $\hat{b}_2 = (-\frac{\sqrt{3}}{2}, \frac{1}{2})$, and $\hat{b}_3 = (0, -1)$, we have $m_0(\mathbf{k}) = m + 2t_z(1 - \cos k_z) + 2t(3 - 2\cos\frac{\sqrt{3}}{2}k_x \cos\frac{1}{2}k_y - \cos k_y)$, $m_1(\mathbf{k}) = 2\sqrt{3}t \sin\frac{\sqrt{3}}{2}k_x \cos\frac{1}{2}k_y$, $m_2(\mathbf{k}) = 2t(\cos\frac{\sqrt{3}}{2}k_x \sin\frac{1}{2}k_y + \sin k_y)$, and $m_3(\mathbf{k}) = 2t_z \sin k_z$. The in-plane and out-of-plane lattice parameters[38] are taken as length units in the above expression, that is $a=c=1$. When $mt_z < 0$ and $mt < 0$, the parametrization defined above[26] and the parametrization in the small \mathbf{k} effective model proposed by Zhang *et al.*[12] describe qualitatively the same physics. With this parametrization, it is easy to see that the model has the inversion symmetry $PH(\mathbf{k})P^{-1} = H(-\mathbf{k})$, where the inversion operator is defined as $P = s_0 \otimes \sigma_1$. [8]

Now, we clarify the differences between models (I) and (II) by their surface states, which is one of the most important signatures of nontrivial topological order in the system. Close to the Γ point in the BZ, we take $m_{i=0,\dots,3}(\mathbf{k}) = \{m + \frac{3}{2}t(k_x^2 + k_y^2) + t_z k_z, 3tk_x, 3tk_y, 2t_z k_z\}$, in which $t > 0$, $t_z > 0$ and $m < 0$. Consider a sample occupying the lower half space $z \leq 0$. The possible surface states localized close to $z = 0$ is searched by solving a set of four coupled second order differential equations

$$H(k_x = k_y = 0, k_z \rightarrow -i\partial_z)\Psi(z) = E\Psi(z), \quad (2)$$

together with the open boundary condition $\Psi(z)|_{z=0} = \Psi(z)|_{z=-\infty} = 0$. [34, 35] $\Psi(z)$ is the four-component eigenvector and E is the energy of the surface mode, respectively. We look for the zero energy states and hence set $E=0$. [34]

For the model (I) with $\Gamma_3 = s_0 \otimes \sigma_2$, the up and down spin degrees of freedom are decoupled from each other. The wave function could thus be written as $\Psi(z) = [u_1(z), u_2(z), u_3(z), u_4(z)]^T = [\chi_{\uparrow}(z), \chi_{\downarrow}(z)]^T$. The two spin components of the zero energy mode satisfy the same equation as (s is \uparrow or \downarrow for the two spin degrees of freedom)

$$[(m - t_z \partial_z^2)\sigma_1 - 2it_z \partial_z \sigma_2]\chi_s(z) = 0. \quad (3)$$

The two degenerate zero energy surface modes for $z \leq 0$ are obtained as

$$\Psi_{\alpha}(z) = C\eta_{\alpha}(e^{z/\xi_+} - e^{z/\xi_-}), \quad (4)$$

where $\alpha=1$ or 2 , C is a normalization constant and $\xi_{\pm}^{-1} = 1 \pm \sqrt{1 + m/t_z}$. $1/\text{Re}[\xi_{\pm}^{-1}]$ ('Re' means taking the real part of a number) are the two penetration depths of the surface modes into the bulk. The two unit vectors are $(\eta_1)_{\beta} = \delta_{\beta 1}$ and $(\eta_2)_{\beta} = \delta_{\beta 3}$, where $\delta_{\alpha\beta}$ is one for $\alpha=\beta$ and zero otherwise. Take $\{\Psi_1, \Psi_2\}$ as the two basis, the effective model for the surface states are obtained by considering the k_x and k_y dependent terms in the original model as perturbations, which are

$$\Delta H_{3D} = \frac{3}{2}t(k_x^2 + k_y^2)\Gamma_0 + 3t(k_x\Gamma_1 + k_y\Gamma_2). \quad (5)$$

Suppose the two basis are normalized, the effective model for the surface states is[12]

$$H_{eff}(\mathbf{k}) = 3t(k_x s_x + k_y s_y), \quad (6)$$

where s_x and s_y are the first and second Pauli matrices. Since the two basis both have definite spin characters, s_x and s_y in the above equation could also be considered as acting in the spin subspace. The most salient feature of this model is that the corresponding surface states has contributions only from the first orbital. When we consider a sample occupying $z \geq 0$, the surface states at $z=0$ would arise only from the second orbital.

We now study model (II) for $\Gamma_3 = s_3 \otimes \sigma_3$. We still consider a sample situated at $z \leq 0$ with the open boundary conditions. Following exactly the same steps as for the first model, we obtain the two degenerate zero energy surface states as

$$\Phi_\alpha = C\eta_\alpha(e^{z/\xi_+} - e^{z/\xi_-}), \quad (7)$$

where $\alpha=1$ or 2 , C is a normalization constant and ξ_\pm are defined identically as above. However, the two unit basis vectors are quite different from the first model and are $\eta_1 = \frac{1}{\sqrt{2}}[1, -i, 0, 0]^T$ and $\eta_2 = \frac{1}{\sqrt{2}}[0, 0, -i, 1]^T$. The two dimensional effective model for the surface states is also a bit different at least formally, which is

$$H_{eff}(\mathbf{k}) = 3t\hat{z} \cdot (\mathbf{k} \times \mathbf{s}) = 3t(k_x s_y - k_y s_x). \quad (8)$$

The Pauli matrices s_x and s_y act in the two fold degenerate basis of the zero energy surface states which both have definite spin characters. For a general two dimensional wave vector, the surface state would be a linear combination of all the four spin-orbital basis.

Thus there are qualitative differences between two models which were used in-discriminatively in the literature for Bi_2Se_3 . [12, 23, 26, 32, 33, 34, 35, 36] While only one orbital contributes to the surface states for model (I), both two orbitals contribute in equal weight to the surface states for model (II). On the other hand, the effective model of the surface states has the same spin-orbital coupled form as the linear k_x and k_y terms in the original three dimensional model for model (I). However, the effective model is changed from $\mathbf{k} \cdot \mathbf{s}$ to $\hat{z} \cdot (\mathbf{k} \times \mathbf{s})$ for model (II). We have verified that, if we change the in-plane spin-orbit coupling of the two models (I) and (II) from $\mathbf{k} \cdot \mathbf{s}$ to $\hat{z} \cdot (\mathbf{k} \times \mathbf{s})$, the resulting effective model of the surface states would have the form $\hat{z} \cdot (\mathbf{k} \times \mathbf{s})$ for model (I) but will be switched to $\mathbf{k} \cdot \mathbf{s}$ for model (II).

Before ending this section, we would like to point out that both the k_z -linear term in $m_3(\mathbf{k})$ and the k_z -square term in $m_0(\mathbf{k})$ are essential to obtain the zero energy surface modes. If we omit the k_z^2 term in $m_0(\mathbf{k})$, it is easy to verify that the gapless surface states no longer exist. This is related to the fact that band inversion is essential to the appearance of nontrivial topological surface states[2, 39], which can only occur in the presence of k_z^2 term for $k_x = k_y = 0$.

III. SUPERCONDUCTING STATE SPECTRAL FUNCTION

A. surface Green's functions in the superconducting state

The realization of the superconducting state in $\text{Cu}_x\text{Bi}_2\text{Se}_3$ [19, 20] has brought about excitement that non-trivial topological superconducting state might be realized in this system, in which topologically protected gapless surface states traverse the bulk superconducting gap.[23, 24, 40] The recent realization of superconducting phase in Bi_2Te_3 under high pressure[21, 22] makes the Bi_2X_3 (X is Se or Te) material a very promising candidate system to realize topologically nontrivial superconducting phases.[23, 24, 40]

The normal state of the topological insulator is marked by the presence of topological surface states inside the bulk gap. These gapless topological surface states are well separated from the bulk conduction band at low energies and become indistinguishable for energies much higher than the conduction band minimum. Depending on the doped charge density the superconducting state could occur with the chemical potential either deep in the bulk conduction band or in the intermediate region where the topological surface states are well separated from the bulk conduction band[20]. In the latter case, the coupling between the continuum bulk states and the isolated topological surface states may cause some new interesting phenomena. Thus this intermediate region is where we will concentrate on below. Furthermore, the actual pairing symmetries of the superconducting $\text{Cu}_x\text{Bi}_2\text{Se}_3$ and Bi_2Te_3 are presently unknown.[19, 20, 21, 22] Thus we will examine cases with different pairing symmetries in the hope to provide clues to identify the pairing symmetry and the role contributed by the topological surface states.

In the following, we will study the surface spectral function to see possible nontrivial topological properties arising from the normal phase topological order which is subject to a certain bulk pairing. The surface spectral function, which could be obtained from the surface Green's function, has been studied by ARPES[20] and STM[25] to give important information on the topological properties of the system. In the superconducting state, we expect to see some surface Andreev bound states if a certain superconducting order is realized in the material.

In the presence of a surface perpendicular to the z -axis, k_x and k_y are good quantum numbers, and k_z is replaced by $-i\partial_z$ as we shall search for surface states. We then discretize the z coordinate and turn the whole sample ($z \leq 0$) with a surface at $z=0$ to a coupled quintuple-layer system. Label each separate quintuple unit with an integer index n , and make the substitutions $\partial_z \psi_n(z) = \frac{1}{2}[\psi_{n+1} - \psi_{n-1}]$ and $\partial_z^2 \psi_n(z) = \psi_{n+1} + \psi_{n-1} - 2\psi_n$ (c is set as length unit along z axis), the Hamiltonian consists now the intra-layer terms and the interlayer hopping terms, $\hat{H} = \hat{H}_\parallel + \hat{H}_\perp$. The intra-layer part of the model is

$\hat{H}_{\parallel} = \sum_{\mathbf{n}\mathbf{k}} \psi_{\mathbf{n}\mathbf{k}}^{\dagger} h_{xy}(\mathbf{k}) \psi_{\mathbf{n}\mathbf{k}}$, in which

$$h_{xy}(\mathbf{k}) = m'_0(\mathbf{k})\Gamma_0 + m_1(\mathbf{k})\Gamma_1 + m_2(\mathbf{k})\Gamma_2. \quad (9)$$

$m_1(\mathbf{k})$ and $m_2(\mathbf{k})$ are the same as those in the bulk model. $m'_0(\mathbf{k})$ is obtained from $m_0(\mathbf{k})$ by first expanding it up to the square term of k_z and then replacing the term proportional to k_z^2 from Ck_z^2 to $2C$.

The inter-layer hopping term is $\hat{H}_{\perp} = \sum_{\mathbf{n}\mathbf{k}} \psi_{\mathbf{n}\mathbf{k}}^{\dagger} h_z \psi_{n+1,\mathbf{k}} + \text{H.c.}$ In terms of the parameterizations of Wang *et al.*[26], we have

$$h_z = -t_z(\Gamma_0 + i\Gamma_3). \quad (10)$$

Since the Γ_3 matrix now appears only in the h_z part of the coupled layers system, the difference between the two models enters only through the interlayer hopping term.

Now introduce superconducting pairing and define the Nambu basis as $\phi_{\mathbf{n}\mathbf{k}}^{\dagger} = [\psi_{\mathbf{n}\mathbf{k}}^{\dagger}, \psi_{n-\mathbf{k}}^T]$. The intra-layer part of the Bogoliubov de Gennes (BdG) Hamiltonian is then $\hat{H}_{\parallel}^{SC} = \sum_{\mathbf{n}\mathbf{k}} \phi_{\mathbf{n}\mathbf{k}}^{\dagger} H_{SC}(\mathbf{k}) \phi_{\mathbf{n}\mathbf{k}}$, in which[41]

$$H_{SC}(\mathbf{k}) = \begin{pmatrix} h_0(\mathbf{k}) & \underline{\Delta}(\mathbf{k}) \\ -\underline{\Delta}^*(-\mathbf{k}) & -h_0^*(-\mathbf{k}) \end{pmatrix}, \quad (11)$$

where $h_0(\mathbf{k}) = h_{xy}(\mathbf{k}) - \mu I_{4 \times 4}$, with μ the chemical potential. $\underline{\Delta}(\mathbf{k})$ is the 4×4 pairing matrix. Ignoring the possibility of interlayer pairing, the interlayer hopping terms are $\hat{H}_{\perp}^{SC} = \sum_{\mathbf{n}\mathbf{k}} \phi_{\mathbf{n}\mathbf{k}}^{\dagger} H_z \phi_{n+1,\mathbf{k}} + \text{H.c.}$, in which

$$H_z = \begin{pmatrix} h_z & 0 \\ 0 & -h_z^* \end{pmatrix}. \quad (12)$$

Once the pairing order is given, the surface spectral function is obtained from the retarded surface Green's functions, which could be calculated in terms of standard transfer matrix method.[42] In the simplest form of the method, the 8×8 retarded surface Green's function $G(\mathbf{k}, \omega)$ is obtained by self-consistent calculation of $G(\mathbf{k}, \omega)$ and a transfer matrix $T(\mathbf{k}, \omega)$ as[26, 42]

$$G^{-1} = g^{-1} - H_z^{\dagger} T, \quad (13a)$$

$$T = G H_z, \quad (13b)$$

where $g = [z I_{8 \times 8} - H_{SC}(\mathbf{k})]^{-1}$ ($z = \omega + i\eta$) is the retarded Green's function for an isolated layer. η is the positive infinitesimal 0^+ , which is replaced by a small positive number in realistic calculations. Self-consistent calculation of the Green's function starts with $G = g$. The surface Green's function could also be obtained in terms of other iteration schemes, such as the algorithm in Ref.[42]. We have found no difference between the results obtained in terms of different iteration schemes.

After the retarded Green's functions are at hand, the spectral function is obtained as

$$A(\mathbf{k}, \omega) = - \sum_{i=1}^4 \text{Im} G_{ii}(\mathbf{k}, \omega) / \pi. \quad (14)$$

Since we have now two orbital and two spin degrees of freedom, there are many possible pairing channels for different possible pairing mechanisms. Realistic theoretical determination of the pairing symmetry requires the knowledge of pairing mechanism and reasonable parameter values, which are both lacking presently.[23] Here we will consider singlet and triplet pairing orders as phenomenological input parameters. Their qualitative differences in spectral functions could help to identify the pairing symmetry from experiments.

B. gap opening in the topological surface states

Before presenting the full spectral function, we first would like to examine what happens to the topological surface states inherited from the normal state[20] upon the formation of a certain bulk pairing. The most salient feature of the topological insulator is the presence of gapless surface states (3D) or edge states (2D).[1, 2, 7, 39] In the case of $\text{Cu}_x\text{Bi}_2\text{Se}_3$, it is found that these surface states in the non-superconducting Bi_2Se_3 persist to the superconducting copper intercalated samples and are well separated from the bulk conduction band and hence well-defined.[19, 20] It is thus an interesting question what would happen to them if a certain pairing forms in the bulk. In this subsection, we give a simple criterion to judge whether a gap would be induced in the topological surface states for an arbitrary bulk pairing.

Suppose the chemical potential lies slightly above the bottom of the bulk conduction band where the topological surface states are well separated and well defined.[20] If a pairing is realized in the topological surface states, it should occur between the two time reversal related states for \mathbf{k} and $-\mathbf{k}$. [17]

We first consider model (I). For our purpose, we would concentrate on the positive energy branch of the topological surface states. When the pairing occurs in the valence band[21, 22], the analysis and conclusion would be similar. Since pairing occurs in the (k_x, k_y) space, we would ignore the z -dependence of the surface modes when analyzing pairing properties. From the basis and the effective model obtained in Sec. II, the two eigenvectors for a certain 2D wave vector are

$$\eta_{\alpha}(\mathbf{k}) = \frac{1}{\sqrt{2}} [1, 0, \alpha \frac{k_+}{k}, 0]^T, \quad (15)$$

where α is '+' ('-') for the upper (lower) branch of the surface states, $k_{\pm} = k_x \pm i k_y$, $k = \sqrt{k_x^2 + k_y^2}$. The annihilation operators of these states are

$$d_{\mathbf{k}\alpha} = \frac{1}{\sqrt{2}} [c_{1\mathbf{k}\uparrow} + \frac{\alpha k_+}{k} c_{1\mathbf{k}\downarrow}] \quad (16)$$

If pairing is induced in the upper surface conduction band at \mathbf{k} , the only possible pairing would be proportional to $d_{\mathbf{k}+}^{\dagger} d_{-\mathbf{k}-}^{\dagger}$. [17] Denote the time-reversal operator as \mathcal{T} . [17,

40] Since $\mathcal{T}c_{1\mathbf{k}\uparrow}^\dagger\mathcal{T}^{-1}=c_{1-\mathbf{k}\downarrow}^\dagger$ and $\mathcal{T}c_{1\mathbf{k}\downarrow}^\dagger\mathcal{T}^{-1}=-c_{1-\mathbf{k}\uparrow}^\dagger$, we have $\mathcal{T}d_{\mathbf{k}+}^\dagger d_{-\mathbf{k}+}^\dagger\mathcal{T}^{-1}=\frac{k_+^2}{k^2}d_{\mathbf{k}+}^\dagger d_{-\mathbf{k}+}^\dagger$. To ensure the time-reversal symmetry of the pairing, the actual pairing should be of the form

$$\begin{aligned}\hat{\Delta}_{SCB}^I(\mathbf{k}) &= \Delta_0 \frac{k_+}{k} d_{\mathbf{k}+}^\dagger d_{-\mathbf{k}+}^\dagger \\ &= \frac{\Delta_0}{2} \left[\frac{k_+}{k} c_{1\mathbf{k}\uparrow}^\dagger c_{1-\mathbf{k}\uparrow}^\dagger - \frac{k_-}{k} c_{1\mathbf{k}\downarrow}^\dagger c_{1-\mathbf{k}\downarrow}^\dagger \right. \\ &\quad \left. + (c_{1\mathbf{k}\downarrow}^\dagger c_{1-\mathbf{k}\uparrow}^\dagger - c_{1\mathbf{k}\uparrow}^\dagger c_{1-\mathbf{k}\downarrow}^\dagger) \right],\end{aligned}\quad (17)$$

where Δ_0 is the real pairing amplitude, which could be an even or odd real function of \mathbf{k} depending on the pairing realized in the bulk. ‘SCB’ is abbreviation for the surface conduction band (the topological surface states). Thus, the surface conduction band only supports the anti-phase $p_x \pm ip_y$ equal-spin triplet pairing and the spin-singlet pairing within orbital 1. No other bulk pairing channels, especially those inter-orbital pairings, would open a gap in the topological surface states within the framework of model (I).

For model (II), the two eigenvectors of the surface states for a certain 2D wave vector are (again, ignoring the z -dependence)

$$\eta_\alpha(\mathbf{k}) = \frac{1}{2} [1, -i, \alpha \frac{k_+}{k}, i\alpha \frac{k_-}{k}]^T, \quad (18)$$

where α is ‘+’ (‘-’) for the upper (lower) branch of the topological surface states. Following the same arguments as for the first model, when the chemical potential cuts the upper branch of these well defined surface states the time reversal invariant pairing is of the form

$$\begin{aligned}\hat{\Delta}_{SCB}^{II}(\mathbf{k}) &= \Delta_0 \frac{k_+}{k} d_{\mathbf{k}+}^\dagger d_{-\mathbf{k}+}^\dagger \\ &= \frac{\Delta_0}{4} \left[\frac{k_+}{k} (c_{1\mathbf{k}\uparrow}^\dagger c_{1-\mathbf{k}\uparrow}^\dagger - c_{2\mathbf{k}\uparrow}^\dagger c_{2-\mathbf{k}\uparrow}^\dagger) \right. \\ &\quad - \frac{k_-}{k} (c_{1\mathbf{k}\downarrow}^\dagger c_{1-\mathbf{k}\downarrow}^\dagger - c_{2\mathbf{k}\downarrow}^\dagger c_{2-\mathbf{k}\downarrow}^\dagger) \\ &\quad + i \frac{k_+}{k} (c_{1\mathbf{k}\uparrow}^\dagger c_{2-\mathbf{k}\uparrow}^\dagger + c_{2\mathbf{k}\uparrow}^\dagger c_{1-\mathbf{k}\uparrow}^\dagger) \\ &\quad + i \frac{k_-}{k} (c_{1\mathbf{k}\downarrow}^\dagger c_{2-\mathbf{k}\downarrow}^\dagger + c_{2\mathbf{k}\downarrow}^\dagger c_{1-\mathbf{k}\downarrow}^\dagger) \\ &\quad + (c_{1\mathbf{k}\downarrow}^\dagger c_{1-\mathbf{k}\uparrow}^\dagger - c_{1\mathbf{k}\uparrow}^\dagger c_{1-\mathbf{k}\downarrow}^\dagger \\ &\quad + c_{2\mathbf{k}\downarrow}^\dagger c_{2-\mathbf{k}\uparrow}^\dagger - c_{2\mathbf{k}\uparrow}^\dagger c_{2-\mathbf{k}\downarrow}^\dagger) \\ &\quad \left. + i (c_{1\mathbf{k}\uparrow}^\dagger c_{2-\mathbf{k}\downarrow}^\dagger + c_{1\mathbf{k}\downarrow}^\dagger c_{2-\mathbf{k}\uparrow}^\dagger - c_{2\mathbf{k}\uparrow}^\dagger c_{1-\mathbf{k}\downarrow}^\dagger - c_{2\mathbf{k}\downarrow}^\dagger c_{1-\mathbf{k}\uparrow}^\dagger) \right].\end{aligned}\quad (19)$$

As in Eq. (17), Δ_0 could be a constant or a real function of \mathbf{k} compatible with the symmetry of one pairing component contained in the above decomposition. Besides the intra-orbital pairing channels active in the model (I), there are two additional inter-orbital pairing channels that are effective in producing a gap in the topological surface states. The last term in the above equation is

just the odd-parity inter-orbital triplet pairing proposed by Fu and Berg[23] as a possible candidate of a topological superconductor to be realized in a superconductor like $\text{Cu}_x\text{Bi}_2\text{Se}_3$.

The clear difference between $\hat{\Delta}_{SCB}^I$ and $\hat{\Delta}_{SCB}^{II}$ makes the distinction between model (I) and model (II) more obvious. Since the gap opening of the surface states is measurable, it is highly desirable to ascertain which model is the correct description of the underlying physics of Bi_2Se_3 and Bi_2Te_3 .

Previously, a simple effective model calculation indicates that no gap opens in the topological surface states for any triplet pairing induced by proximity effect on the surface of a topological insulator.[41] However, our analysis above indicates that if the proximity induced triplet pairing is compatible with any of the triplet components explicit in $\hat{\Delta}_{SCB}^I$ ($\hat{\Delta}_{SCB}^{II}$) for model I (model II), then a full pairing gap could still be opened in the topological surface states. Note that the real gap opening pattern in the topological surface states also depends on Δ_0 .

Except for the pairing channels explicit in $\hat{\Delta}_{SCB}^I$ for model (I) and $\hat{\Delta}_{SCB}^{II}$ for model (II), no other bulk pairing could open a gap in the topological surface states. The existence of surface Andreev bound states depends on whether or not a gap opens in the topological surface states. We clarify this matter in the next section.

C. spectral function for typical pairing symmetries

Observation of superconductivity in $\text{Cu}_x\text{Bi}_2\text{Se}_3$ brings about anticipation that nontrivial topological superconducting states might be realized in this material. The topological superconductor is defined as a state with a full pairing gap in the bulk and nontrivial gapless Andreev bound states on the surface.[23]

Possible pairings realizable in a system depend on the symmetry of the system and the specific pairing mechanism. In the case of pairing induced by short range electron density-density interactions, Fu and Berg identified four possible pairing channels.[23] However, if the pairing is induced by more long-range interactions, such as the electron-phonon interaction, other pairing channels (e.g., in which the pairing potential is \mathbf{k} dependent) would also be possible. In the following we would analyze several typical pairings and compare results of the two different models. In each case, there are three typical situations as regards to the position of the chemical potential μ : (1) μ lies in the bulk gap; (2) μ lies above but close to the bottom of the bulk conduction band, where the topological surface states are well separated from the continuum bulk conduction band; (3) μ lies far above the bulk conduction band bottom, where the surface states have merged into the continuum conduction band. While the latter two cases are relevant to the superconducting state of $\text{Cu}_x\text{Bi}_2\text{Se}_3$ [19, 20], the first case could be regarded as mimicking the proximity effect from an external superconductor.[17, 18, 41] In this paper we

would focus on the latter two situations. When the chemical potential lies in the valence band[21, 22], the results should be qualitatively similar for the same type of bulk pairing.

Follow Wang *et al.*[26], the model parameters are taken as $t=t_z=0.5$, $m=-0.7$ in most cases. 0.7 is half of the bulk band gap. The width of the bulk conduction band at $k_x=k_y=0$ is $2(2t_z - |m|)=0.6$. The small positive number η in the Green's functions is taken as 10^{-4} .

- *even-parity intra-orbital singlet pairing* First, we study the simplest possible pairing denoted by $\underline{\Delta}(\mathbf{k})=i\Delta_0 s_2 \otimes \sigma_0$. Spectral functions for the two different models are the same for this pairing, so only one is presented in Fig. 1. Here and in the following, the degree of darkness indicates the intensity of the spectrum. The continuum portions of spectrum are contributions from the bulk states, which have small finite amplitudes on the surface. Henceforth, they would be called bulk conduction band for simplicity. The contributions from the topological surface states are somewhat speckled because we have taken a finite grid in the (\mathbf{k}, ω) plane to calculate the spectral function. When the grid points are taken to be very dense, contributions from the topological surface states will also become smooth. To see the qualitative behavior more clearly, a reasonably large pairing amplitude $\Delta_0=0.1$ is considered.[20] The result is nearly identical in the ΓK direction (along k_x axis) and the ΓM direction (along k_y axis) of the 2D reduced Brillouin zone (BZ). The topological surface states of both two models open a gap, which are consistent with the analysis of the previous subsection. Since no Andreev bound state exists, this pairing is topologically trivial. The other intra-orbital singlet pairings with a \mathbf{k} -dependent Δ_0 , which is an even function of \mathbf{k} could also be considered, such as the $d_{x^2-y^2}$ -wave pairing. In these cases, there would be line nodes along the nodal directions of the pairing gap.

- *even-parity inter-orbital singlet pairing* Since there are now two orbits, another singlet pairing exists in the inter-orbital channel. The pairing matrix for the s -wave case is $\underline{\Delta}(\mathbf{k})=i\Delta_0 s_2 \otimes \sigma_1$. The corresponding spectral functions presented in Fig. 2 for this pairing are still identical for the two models. They differ from the spectra of the former intra-orbital pairing channel in at least two aspects. First, no gap opens in the topological surface states, which is in agreement with the criterion proposed in the previous subsection. Second, though a full gap also opens in the continuum part of the spectrum, it is not constant and shows some \mathbf{k} dependence. As shown in Fig. 2(b), the continuum part of the spectrum even nearly closes at some special wave vectors for certain parameters. Another interesting feature is the strong redistribution of spectral weight between the continuum conduction band and the topological surface states. Some weight in the bulk conduction band part of the surface spectrum above the chemical potential is depleted and transferred to the topological surface states below the chemical potential. This redistribution arises from the particle hole mixing induced by the presence of bulk su-

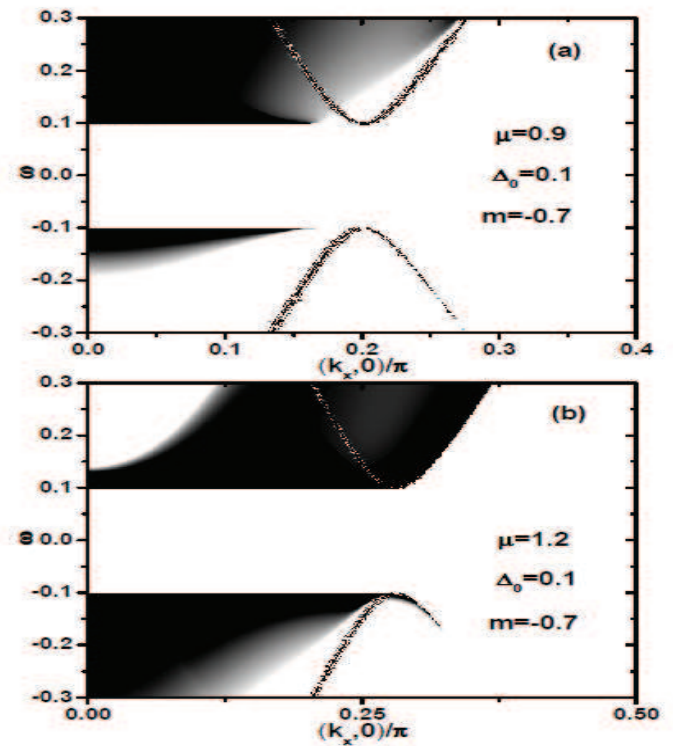


FIG. 1: Spectral function for even-parity intra-orbital s -wave pairing, for two typical parameter sets for which the topological surface states at the chemical potential (a) are well separated from the bulk conduction band and (b) merges into the bulk conduction band. The two models give identical results for this pairing. Spectrum along other directions (crossing the Γ point) are qualitatively identical.

perconducting pairing. As would see below, a similar feature is present for each bulk pairing that does not open a gap in the topological surface states.

- *odd-parity inter-orbital triplet pairing* We now consider the odd-parity inter-orbital triplet pairing channel, proposed by Fu and Berg as a candidate for possible nontrivial topological superconducting states in $\text{Cu}_x\text{Bi}_2\text{Se}_3$. [23] The pairing matrix is $\underline{\Delta}(\mathbf{k})=\Delta_0 s_1 \otimes \sigma_2$. As was shown in Fig. 3, the spectral functions for the two models differ greatly. When the chemical potential is close to bottom of the bulk conduction band, the surface conduction band is still gapless for model (I) but opens a gap for model (II), in agreement with the analysis in the above subsection. Another essential difference is the existence or not of Andreev bound states. For model (I), a band of Andreev bound states appears inside of the insulating gap of the continuum which continuously connects to the topological surface states. While for model (II), there is a point node at $(0, 0)$, no Andreev bound state exists inside of the gap region. When the chemical potential is increased to the position where the surface conduction band has almost merged into the continuum part of the surface spectrum (corresponding to contribution from the bulk conduction band), surface spectra

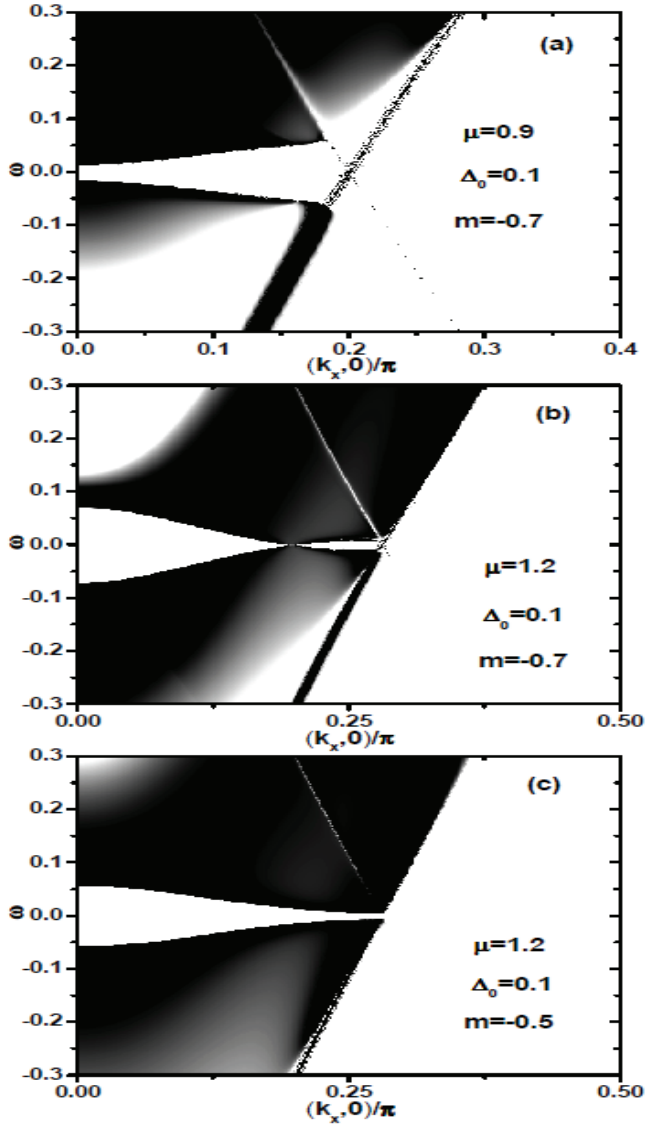


FIG. 2: Spectral function for even-parity inter-orbital s -wave pairing, for three sets of parameters for which at the chemical potential (a) the topological surface states are well separated from the bulk conduction band, (b) the topological surface states are almost merged into the bulk conduction band, and (c) the topological surface states are well merged into the bulk conduction band. The two models give identical results for this pairing. Spectrum along other directions (crossing the Γ point) are qualitatively identical.

for the two models are as shown in Fig. 4. Since now there is no well separated surface conduction band, a full gap opens also for the model (I). However, a band of Andreev bound states still exists. When we further increase the chemical potential to $\mu > 1.3$ (for $m=-0.7$), there is no state close to the Γ point, then there would be no Andreev bound state even for model (I). A strong redistribution of spectral weight arising from the particle hole mixing between the continuum bulk conduction band and the topological surface states is observed in

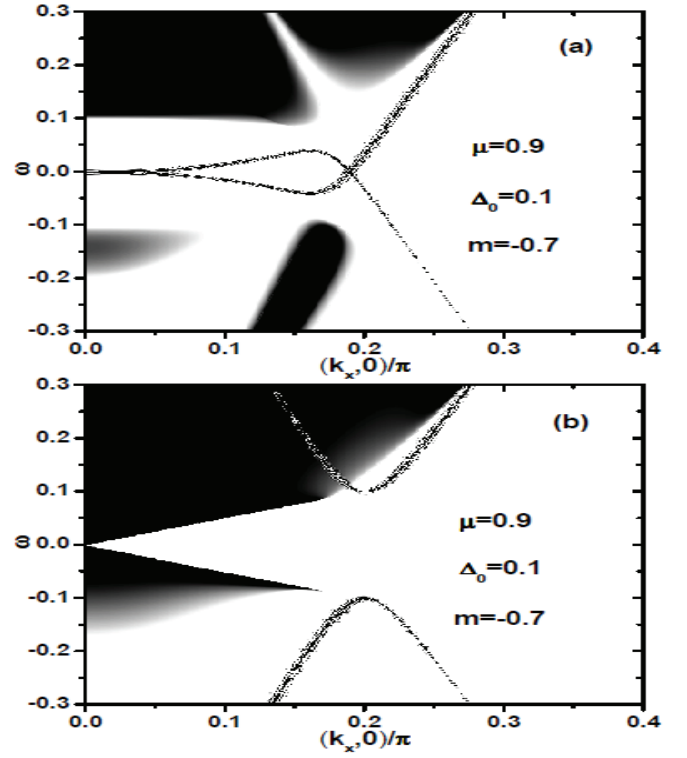


FIG. 3: Spectral function for odd-parity inter-orbital triplet pairing in the opposite spin pairing channel, for (a) model (I) and (b) model (II). As shown are the cases for which the topological surface states are well separated from the bulk conduction band at the chemical potential. The parameters are as shown on the figures. Spectrum along other directions (crossing the Γ point) are qualitatively identical.

results for model (I).

Besides the pairing studied above, there are also other odd-parity pairings. Since they are possibly related with nontrivial topological superconducting phases, we analyze several of them in the following.

- *odd-parity intra-orbital singlet pairing* In this case, every orbit pairs into a spin-singlet, but the two orbits has a relative π phase difference and is hence odd in parity.[23] The pairing matrix is denoted as $\underline{\Delta}(\mathbf{k})=i\Delta_0 s_2 \otimes \sigma_3$. The corresponding spectral functions for the two models are presented in Figs. 5(a) and 5(b) for chemical potential close to the bottom of the bulk conduction band and thus the topological surface state is well defined. A comparison with the previous pairing, shown in Figs. 3 and 4, indicates that the results are interchanged between the two models. Gap opening in the topological surface states again follows the expectation from the previous subsection. The Andreev bound states in the bulk band gap for the second model again connect continuously to the protected topological surface states. The behaviors for higher chemical potentials, as shown in Figs. 5(c) and 5(d), are similar to that of the previous pairing shown in Fig. 4 with the two models interchanged.

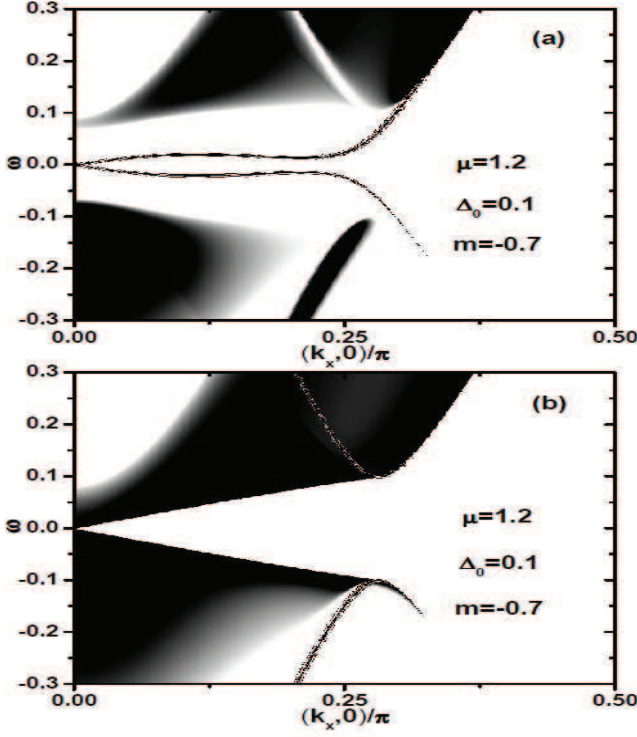


FIG. 4: Spectral function for odd-parity inter-orbital triplet pairing in the opposite spin pairing channel, for (a) model (I) and (b) model (II). As shown are the cases for which the topological surface states are merged into the bulk conduction band at the chemical potential. The parameters are as shown on the figures. Spectrum along other directions (crossing the Γ point) are qualitatively identical.

- *odd-parity inter-orbital equal-spin triplet pairing* Another interesting possibility is the equal-spin pairing channel. Here we consider the two fold degenerate inter-orbital pairing channels as proposed by Fu and Berg.[23] This kind of pairing could be favored by interorbital ferromagnetic Heisenberg interactions.[43] The two independent choices for the pairing matrix are $\underline{\Delta}^{(1)}(\mathbf{k}) = i\Delta_0 s_0 \otimes \sigma_2$ and $\underline{\Delta}^{(2)}(\mathbf{k}) = \Delta_0 s_3 \otimes \sigma_2$. For these pairings, it is easy to see that no gap opens in the topological surface states for both models. Since results for the two models are identical, we only show those for the model (I). As shown in Fig. 6 for $\underline{\Delta}^{(1)}(\mathbf{k})$, a peculiar anisotropic Andreev bound state structure is observed. An important difference of this pairing from the above odd-parity pairing channels is that it is anisotropic with respect to k_x and k_y . Though the bulk dispersion is gapless in the $k_y k_z$ ($k_x k_z$) plane for $\underline{\Delta}^{(1)}(\mathbf{k})$ ($\underline{\Delta}^{(2)}(\mathbf{k})$), there is still a band of Andreev bound states for the wave vectors smaller than k_F where a gap opens. The peculiar feature of the Andreev bound states along k_y (k_x) for $\underline{\Delta}^{(1)}(\mathbf{k})$ ($\underline{\Delta}^{(2)}(\mathbf{k})$) is that they are dispersion-less (that is, completely flat).

Besides the Andreev bound states within the gap, the

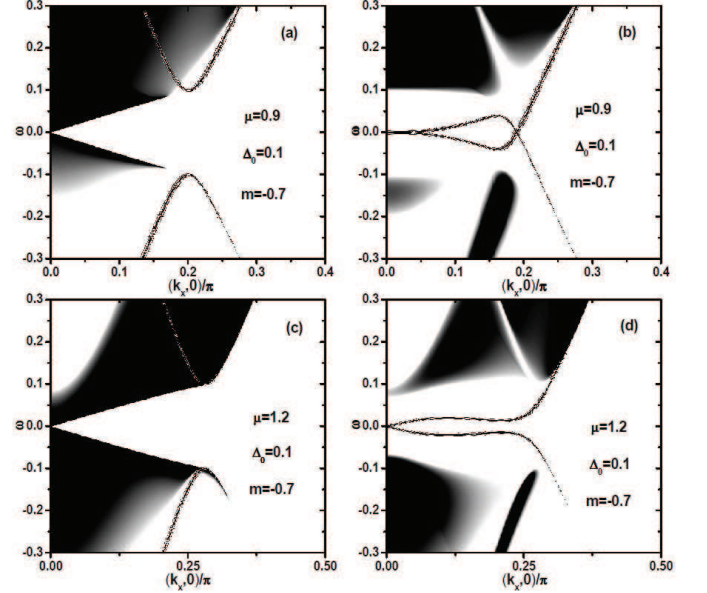


FIG. 5: Spectral function for odd-parity intra-orbital s -wave pairing, for model (I) ((a) and (c)) and model (II) ((b) and (d)). For (a) and (b) ((c) and (d)), the topological surface states are well separated from (merged into) the bulk conduction band at the chemical potential. Spectrum along other directions (crossing the Γ point) are qualitatively identical.

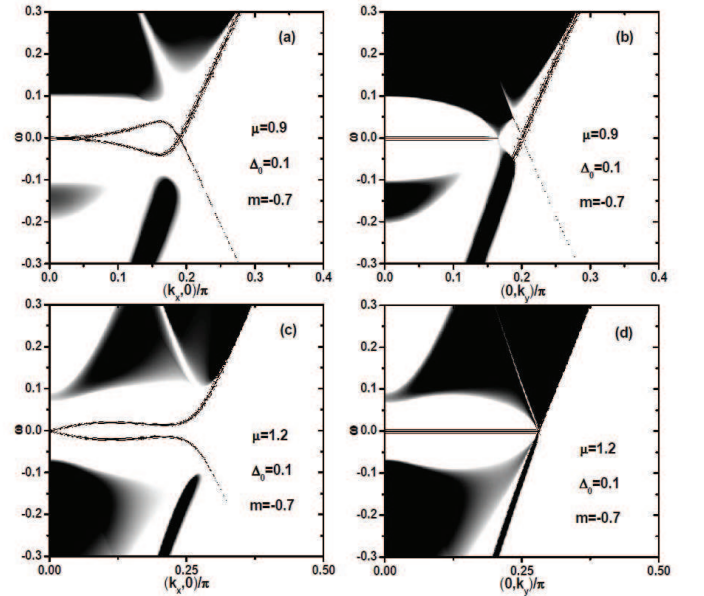


FIG. 6: Spectral function for odd-parity inter-orbital triplet pairing in the equal spin pairing channel, for model (I) and $\underline{\Delta}^{(1)}(\mathbf{k}) = i\Delta_0 s_0 \otimes \sigma_2$. (a) and (c) are along the k_x direction while (b) and (d) are along the k_y direction. The parameters are as shown on the figure.

redistribution of spectral weights arising from the particle hole mixing is also very interesting. An important feature is the appearance of a linear band beyond the Fermi momentum and below the chemical potential, existing as a particle hole symmetric band of the original topological surface states in the normal phase. Once a bulk superconducting pairing forms in the topological insulator itself (and not in the intercalated copper) in $\text{Cu}_x\text{Bi}_2\text{Se}_3$, such a linear dispersive band is always there, no matter a gap opens or not in the topological surface states. To see the above feature more clearly, we show in Figs. 7(a) and 7(b) the energy distribution curves (EDC) for several typical wave vectors for two typical pairings and parameter sets, which are same as those of Figs. 1(a) and 3(a), respectively. The linear band mentioned above appears as a well defined peak slightly below the chemical potential. As the wave vector increases and shifts away from the Fermi momentum, the peak deviates linearly from the chemical potential and the height and width of it both decrease rapidly, which is in agreement with the fact that superconducting pairing forms only close to the chemical potential. The integrated weight of the linearly dispersive peaks in Figs. 7(a) and 7(b) are shown in Fig. 7(c), as a function of the wave vector. If the gap in the superconductors realized from a topological insulator is larger than what is reported in Ref. [20], the above linear dispersive structure in the EDC could be detectable by ARPES for the wave vectors close enough to the Fermi momentum.[19, 20] Then this well defined peak structure arising from the topological surface states could be used as a good indicator of the formation of superconducting correlation in Bi_2Se_3 and the involvement of the topological surface states in the superconducting phase.

From the above results for five different pairing symmetries, we observe a simple rule for the existence of nontrivial surface Andreev bound states. For odd-parity pairings, when a full gap opens in the continuum part of the surface spectrum but no gap opens in the topological surface states, a band of surface Andreev bound states would arise which traverses the bulk pairing gap. This criterion is verified also by calculations for other superconducting pairings not presented here. The results in this subsection are summarized in Table I.

D. the surface Andreev bound states

For some superconducting pairings, such as the $p \pm ip$ wave pairing, it was known that Majorana fermions exist as gapless surface or edge modes.[40] According to an argument by Linder *et al*, all zero energy Andreev bound states emerging from the nondegenerate (that is, on each surface) topological surface states should be Majorana fermions.[41] As regards our case, in the parameter region where the topological surface states are well separated from the bulk conduction band, one observation is that the surface Andreev bound states in the gap region connect continuously to the topological surface states in-

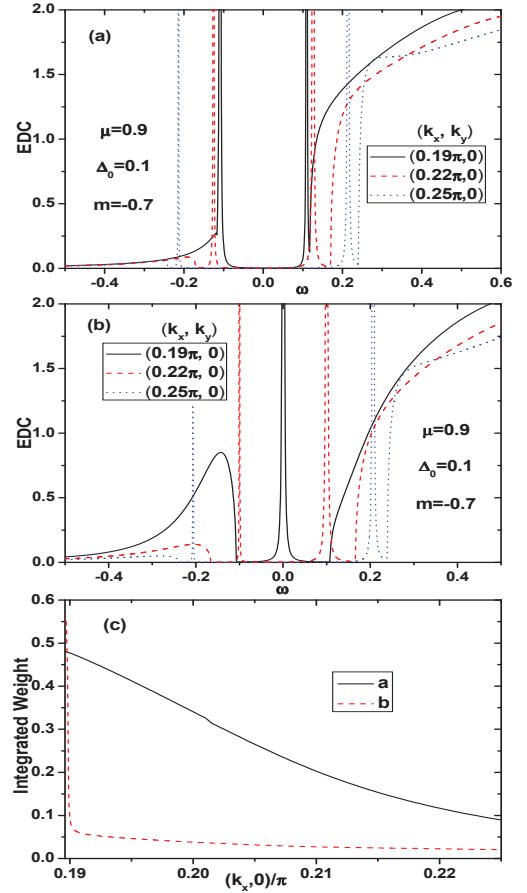


FIG. 7: EDC for three typical wave vectors for (a) even-parity intra-orbital singlet pairing (with parameters same as in Fig. 1(a)) and (b) odd-parity inter-orbital triplet pairing (with parameters same as in Fig. 3(a)) within model (I). The parameters are as shown on the figures. (c) The integrated weight of the linearly dispersive peaks slightly below the chemical potential with parameters corresponding to (a) and (b), respectively.

herited from the normal phase (e.g., Fig. 3(a)). Since the topological surface states are spin polarized helical and nondegenerate, the surface Andreev bound states on each surface should also be nondegenerate. Then according to the arguments by Linder *et al*[41], the zero energy Andreev bound states presented in the above section should also be Majorana fermions.

To see more clearly the properties of the surface Andreev bound states, we perform numerical calculations on a finite layer superconducting film. As an example, we will analyze the odd-parity inter-orbital triplet pairing channel described by $\Delta(\mathbf{k}) = \Delta_0 s_1 \otimes \sigma_2$, within model (I). Fig. 8(a) shows the dispersion for a fifty layer film. It reproduces all the basic features in the spectral function (see Fig. 3(a)). Enlargement of the low energy dispersion (Fig. 8(b)) shows that dispersion of the surface Andreev bound states is linear close to the Γ point. For all the bulk pairings studied above, the dispersion for the su-

TABLE I: Summary of results for the bulk pairings considered explicitly in the present work. Results for two models, (I) and (II), are compared. ‘TSS’ and ‘ABS’ are the abbreviations for ‘topological surface states’ and ‘Andreev bound states’, respectively. ‘+’ and ‘-’ means the even-parity and odd-parity pairings. For ‘Gap in TSS’, ‘Y’ and ‘N’ represents that a gap could and could not open in the topological surface states. For ‘ABS’, ‘Y’ and ‘N’ denotes that Andreev bound states exist and do not exist on the surface for a certain bulk pairing.

$\Delta(\mathbf{k})$	$is_2 \otimes \sigma_0$	$is_2 \otimes \sigma_1$	$s_1 \otimes \sigma_2$	$is_2 \otimes \sigma_3$	$is_0 \otimes \sigma_2$
P	+	+	-	-	-
Gap in TSS: (I)	Y	N	N	Y	N
Gap in TSS: (II)	Y	N	Y	N	N
ABS: (I)	N	N	Y	N	Y
ABS: (II)	N	N	N	Y	Y

perconducting film reproduces well the features of the corresponding spectral function. Figure 9(a) shows the wave function amplitudes for the surface state localized on the top several layers. The corresponding behavior for the topological surface states in the normal phase is presented in Fig. 9(b). The decay behavior of the surface bound states into the bulk in Fig. 9(a) is seen to change continuously from oscillatory exponential decay in the gap region[23] to monotonic exponential decay outside the gap region. That is, the state changes from particle-hole mixed superconducting quasiparticle to the topological surface states in the normal phase.

In this paper, we have always been discussing a homogeneous phase both in the bulk and on the surface. However, in the presence of exotic surface excitations as vortices, novel Majorana fermion modes may appear in the vortex core even for bulk pairings with no surface Andreev bound states. There have already been many papers focusing on this possibility, which usually start from the effective model.[43, 44, 45]

The Andreev bound states that appear in many different superconducting pairings as shown above confirm the idea that superconducting states realized in a topological insulator are very probable to have nontrivial topological characters. The Andreev bound states, if exist, should be easily detectable in a tunneling type experiments as a well defined zero energy peak. Another way to detect the Majorana fermions as zero energy Andreev bound states is to take advantage of the various phase sensitive transport devices proposed to produce and manipulate the Majorana fermions.[17, 46]

IV. SUMMARY

In this paper, we have discussed the surface spectral function of superconductors realized from a topological insulator, such as the copper-intercalated Bi_2Se_3 . These functions are calculated by projecting bulk states to the surface for two different models used previously for the

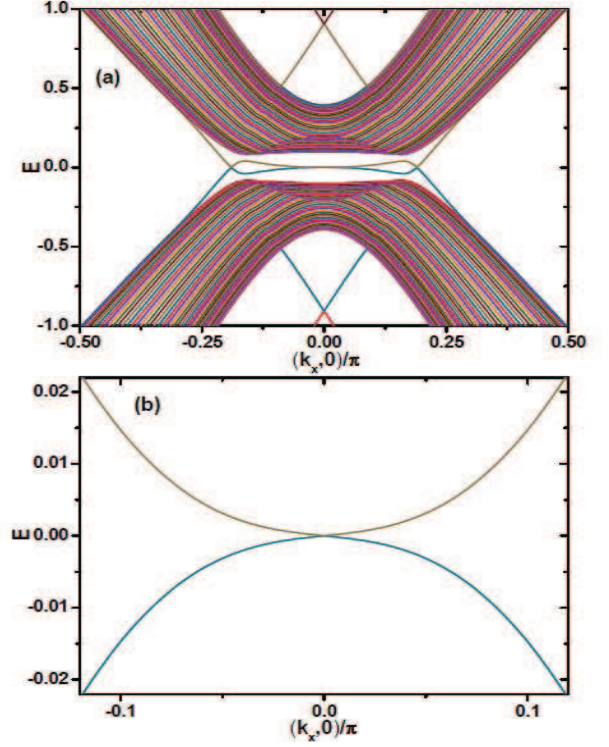


FIG. 8: (a) Dispersion of a fifty layer superconductor emerging from model (I) and for the odd-parity inter-orbital triplet pairing $\Delta(\mathbf{k})=\Delta_0 s_1 \otimes \sigma_2$. Parameters used are $\mu=0.9$, $\Delta_0=0.1$, and $m=-0.7$. (b) An enlargement of the small wave vector and low energy part of (a).

topological insulator. Dependence of the surface spectra on the symmetry of the bulk pairing order parameter are discussed with particular emphasis on the odd-parity pairing. When an odd-parity pairing opens a full gap in the bulk, but not for the topological surface states, zero energy Andreev bound states are shown to appear on the surface. When the topological surface states are well separated from the bulk conduction band, the redistribution of spectral weight induced by the onset of superconductivity produces a linearly dispersive peak structure beyond the Fermi momentum and below the chemical potential. It is proposed as a criterion for confirming that superconductivity occurs in the Bi_2Se_3 (and not in copper) and the topological surface states are involved in the superconducting phase. The zero energy surface Andreev bound states are argued to be Majorana fermions.

Acknowledgments

We thank Peter Thalmeier for helpful discussions. This work was supported by the NSC Grant No. 98-2112-M-001-017-MY3. Part of the calculations was performed in the National Center for High-Performance Computing in Taiwan.

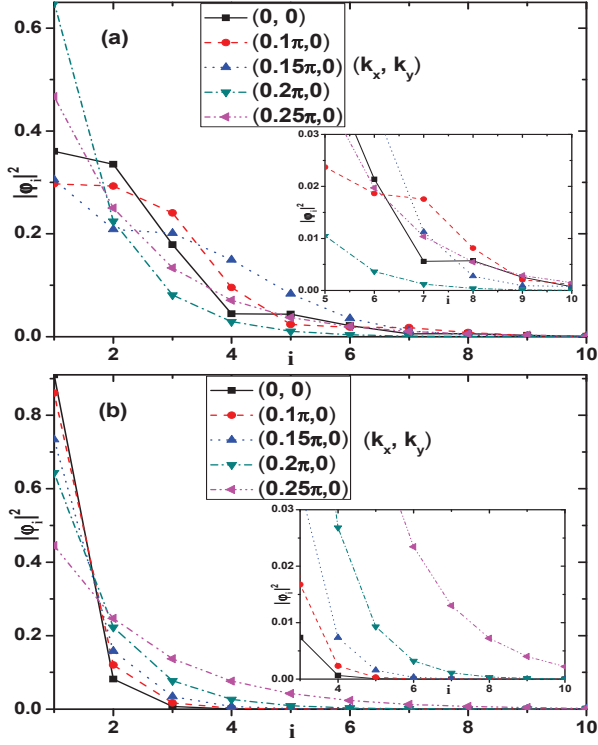


FIG. 9: (a) Decay of the wave function amplitude with layer number for the surface Andreev bound states localized on the top several layers, results are obtained for the superconducting state emerging from model (I) and for the odd-parity inter-orbital triplet pairing $\underline{\Delta}(\mathbf{k}) = \Delta_0 s_1 \otimes \sigma_2$. The parameters are $\mu = 0.9$, $\Delta_0 = 0.1$, and $m = -0.7$. The Fermi wave vector in the k_x direction is about 0.19π . (b) Decay of the wave function amplitude with layer number for the topological surface states localized on the top several layers, for the normal states of model (I) with $m = -0.7$. The two insets show enlargements of the small amplitude regions of the two figures.

-
- [1] C. L. Kane and E. J. Mele, Phys. Rev. Lett. **95**, 146802 (2005); *ibid* **95**, 226801 (2005).
[2] B. Andrei Bernevig, Taylor Hughes, and Shou-Cheng Zhang, Science **314**, 1757 (2006).
[3] D. N. Sheng, Z. Y. Weng, L. Sheng, and F. D. M. Haldane, Phys. Rev. Lett. **97**, 036808 (2006).
[4] Markus König, Steffen Wiedmann, Christoph Brüne, Andreas Roth, Hartmut Buhmann, Laurens W. Molenkamp, Xiao-Liang Qi, Shou-Cheng Zhang, Science **318**, 766 (2007).
[5] J. E. Moore and L. Balents, Phys. Rev. B **75**, 121306 (2007).
[6] R. Roy, arXiv:0607531.
[7] Liang Fu, C. L. Kane, and E. J. Mele, Phys. Rev. Lett. **98**, 106803 (2007).
[8] Liang Fu and C. L. Kane, Phys. Rev. B **76**, 045302 (2007).
[9] D. Hsieh, D. Qian, L. Wray, Y. Xia, Y. S. Hor, R. J. Cava, and M. Z. Hasan, Nature **452**, 970 (2008).
[10] Xiao-Liang Qi, Taylor L. Hughes, and Shou-Cheng Zhang, Phys. Rev. B **78**, 195424 (2008).
[11] Y. Xia, D. Qian, D. Hsieh, L. Wray, A. Pal, H. Lin, A. Bansil, D. Grauer, Y. S. Hor, R. J. Cava, and M. Z. Hasan, Nature Phys. **5**, 398 (2009).
[12] Haijun Zhang, Chao-Xing Liu, Xiao-Liang Qi, Xi Dai, Zhong Fang, and Shou-Cheng Zhang, Nature Phys. **5**, 438 (2009).
[13] M. Z. Hasan and C. L. Kane, Rev. Mod. Phys. **82**, 3045 (2010).
[14] Xiao-Liang Qi and Shou-Cheng Zhang, arXiv:1008.2026.
[15] Andreas P. Schnyder, Shinsei Ryu, Akira Furusaki, and Andreas W. W. Ludwig, Phys. Rev. B **78**, 195125 (2008).
[16] Frank Wilczek, Nature Phys. **5**, 614 (2009).
[17] Liang Fu and C. L. Kane, Phys. Rev. Lett. **100**, 096407 (2008); *ibid*, Phys. Rev. Lett. **102**, 216403 (2009).
[18] Jay D. Sau, Roman M. Lutchyn, Sumanta Tewari, and S. Das Sarma, Phys. Rev. B **82**, 094522 (2010).
[19] Y. S. Hor, A. J. Williams, J. G. Checkelsky, P. Roushan, J. Seo, Q. Xu, H. W. Zandbergen, A. Yazdani, N. P. Ong,

- and R. J. Cava, Phys. Rev. Lett. **104**, 057001 (2010).
- [20] L. Andrew Wray, Su-Yang Xu, Yuqi Xia, Yew San Hor, Dong Qian, Alexei V. Fedorov, Hsin Lin, Arun Bansil, Robert J. Cava and M. Zahid Hasan, Nature Phys. 1762 (2010).
- [21] J. L. Zhang, S. J. Zhang, H. M. Weng, W. Zhang, L. X. Yang, Q. Q. Liu, S. M. Feng, X. C. Wang, R. C. Yu, L. Z. Cao, L. Wang, W. G. Yang, H. Z. Liu, W. Y. Zhao, S. C. Zhang, X. Dai, Z. Fang, C. Q. Jin, arXiv: 1009.3691v1.
- [22] Chao Zhang, Liling Sun, Zhaoyu Chen, Xingjiang Zhou, Qi Wu, Wei Yi, Jing Guo, Xiaoli Dong, and Zhongxian Zhao, arXiv: 1009.3746v1.
- [23] Liang Fu and Erez Berg, Phys. Rev. Lett. **105**, 097001 (2010).
- [24] Masatoshi Sato, Phys. Rev. B **81**, 220504(R) (2010); *ib id* **79**, 214526 (2009).
- [25] Zhanybek Alpichshev, J. G. Analytis, J.-H. Chu, I. R. Fisher, Y. L. Chen, Z. X. Shen, A. Fang, and A. Kapitulnik, Phys. Rev. Lett. **104**, 016401 (2010).
- [26] Qiang-Hua Wang, Da Wang, and Fu-Chun Zhang, Phys. Rev. B **81**, 035104 (2010).
- [27] D. Hsieh, Y. Xia, D. Qian, L. Wray, J. H. Dil, F. Meier, J. Osterwalder, L. Patthey, J. G. Checkelsky, N. P. Ong, A. V. Fedorov, H. Lin, A. Bansil, D. Grauer, Y. S. Hor, R. J. Cava, and M. Z. Hasan, Nature **460**, 1101 (2009).
- [28] Binghai Yan, Chao-Xing Liu, Hai-Jun Zhang, Chi-Yung Yam, Xiao-Liang Qi, Thomas Frauenheim, and Shou-Cheng Zhang, EPL **90**, 37002 (2010).
- [29] K. Kuroda, M. Ye, A. Kimura, S. V. Ereemeev, E. E. Krasovskii, E. V. Chulkov, Y. Ueda, K. Miyamoto, T. Okuda, K. Shimada, H. Namatame, and M. Taniguchi, Phys. Rev. Lett. **105**, 146801 (2010).
- [30] Zhi Ren, A. A. Taskin, Satoshi Sasaki, Kouji Segawa, and Yoichi Ando, Phys. Rev. B **82**, 241306 (2010).
- [31] Su-Yang Xu, L. A. Wray, Y. Xia, R. Shankar, A. Petersen, A. Fedorov, H. Lin, A. Bansil, Y. S. Hor, D. Grauer, R. J. Cava, M. Z. Hasan, arXiv:1007.5111.
- [32] Rundong Li, Jing Wang, Xiao-Liang Qi and Shou-Cheng Zhang, Nature Phys. **6**, 284 (2010).
- [33] Chao-Xing Liu, Haijun Zhang, Binghai Yan, Xiao-Liang Qi, Thomas Frauenheim, Xi Dai, Zhong Fang, and Shou-Cheng Zhang, Phys. Rev. B **81**, 041307(R) (2010).
- [34] Chao-Xing Liu, Xiao-Liang Qi, Haijun Zhang, Xi Dai, Zhong Fang, and Shou-Cheng Zhang, Phys. Rev. B **82**, 045122 (2010).
- [35] Hai-Zhou Lu, Wen-Yu Shan, Wang Yao, Qian Niu, and Shun-Qing Shen, Phys. Rev. B **81**, 115407 (2010).
- [36] Wen-Yu Shan, Hai-Zhou Lu, and Shun-Qing Shen, New J. Phys. **12**, 043048 (2010).
- [37] Liang Fu, Phys. Rev. Lett. **103**, 266801 (2009).
- [38] P. Larson, V. A. Greanya, W. C. Tonjes, Rong Liu, S. D. Mahanti, and C. G. Olson, Phys. Rev. B **65**, 085108 (2002).
- [39] Xiao-Liang Qi and Shou-Cheng Zhang, Phys. Today **63**, No. 1, 33 (2010).
- [40] Xiao-Liang Qi, Taylor L. Hughes, and Shou-Cheng Zhang, Phys. Rev. B **81**, 134508 (2010).
- [41] Jacob Linder, Yukio Tanaka, Takehito Yokoyama, Asle Sudbø, and Naoto Nagaosa, Phys. Rev. Lett. **104**, 067001 (2010).
- [42] M. P. López Sancho, J. M. López Sancho and J. Rubio, J. Phys. F: Met. Phys. **14**, 1205 (1984); *ib id*, J. Phys. F: Met. Phys. **15**, 851 (1985).
- [43] Luiz Santos, Titus Neupert, Claudio Chamon, and Christopher Mudry, Phys. Rev. B **81**, 184502 (2010).
- [44] Xiao-Liang Qi, Taylor L. Hughes, S. Raghu, and Shou-Cheng Zhang, Phys. Rev. Lett. **102**, 187001 (2009).
- [45] Pavan Hosur, Pouyan Ghaemi, Roger S. K. Mong, and Ashvin Vishwanath, arXiv: 1012.0330v1.
- [46] K. T. Law, Patrick A. Lee, and T. K. Ng, Phys. Rev. Lett. **103**, 237001 (2009).